



# FABRICATION AND CHARACTERIZATION OF KETOPROFEN-LOADED NANOSUSPENSION USING A CENTRAL COMPOSITE DESIGN

Mahesh N. Sanas.<sup>1\*</sup>, Tejas S. Pachpute<sup>2\*</sup>

Article History: Received: 23.03.2023

Revised: 05.05.2023

Accepted: 19.06.2023

## Abstract

The present study endeavours practically for the formulation of ketoprofen-loaded nanosuspension. A central composite design was used for the influence of the formulation variables on the responses. ANOVA was applied to evaluate statistical significance ( $p < 0.05$ ). The prepared nanosuspension was optimized and subsequently lyophilized to obtain the dry nanosuspension. The dry powder of nanosuspension was further analysed using DSC and PXRD. The drug particles were transformed during the processing of the nanosuspension and found to be in amorphous form. The compatibility was studied by the FTIR. The in vitro evaluation was performed and 98 % sustained release was found up to 24 h. In conclusion, CCD is employed to find the effect of variables on their response to the nano formulation. Thus, nanosuspension is the best nano formulation that improves solubility and bioavailability respectively. Thus, the KTP-loaded nanosuspension improves its solubility and bioavailability. Thus, the prepared nanosuspension is cost-effective and safe to improve solubility and bioavailability.

**Keywords:** Ketoprofen; Central Composite Design; Bioavailability; Nanosuspension.

<sup>1,2</sup>Department of Pharmaceutics, Alwar Pharmacy College, Sunrise University, Alwar, Rajasthan, India

## #Equal Contribution

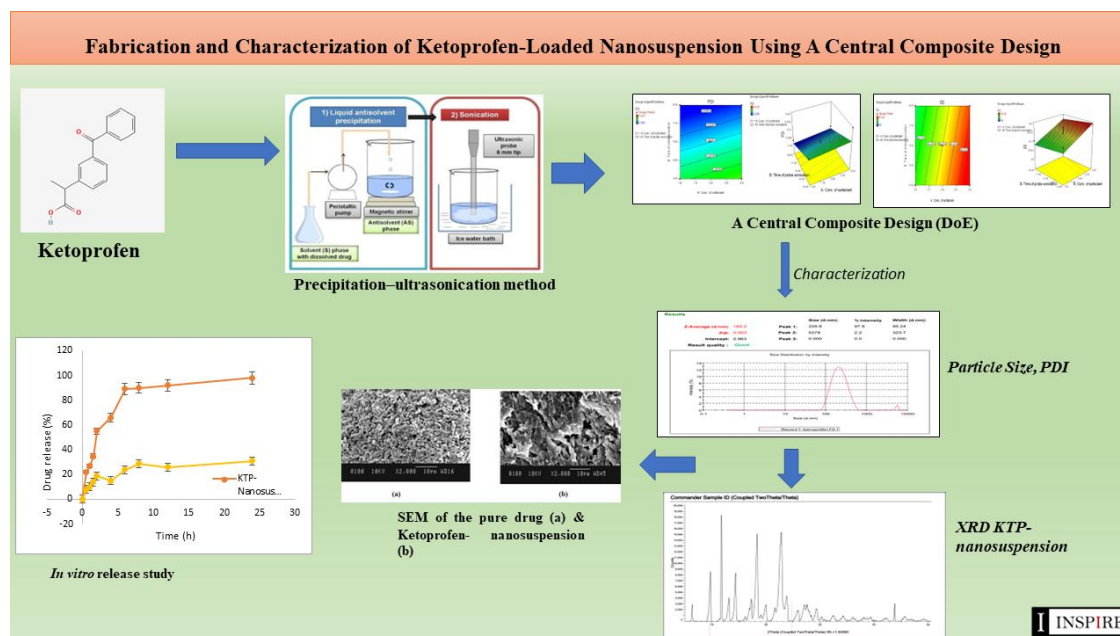
## \*Corresponding Author

Mahesh N. Sanas<sup>1\*</sup>

Department of Pharmaceutics, Alwar Pharmacy College, Sunrise University, Alwar, Rajasthan, India

Email ID: [sanasmahesh1983@gmail.com](mailto:sanasmahesh1983@gmail.com)

DOI: 10.31838/ecb/2023.12.6.65



## 1. INTRODUCTION

Ketoprofen (KTP) is a potent, classical NSAID of the aryl propionic acid class. Classical NSAIDs inhibit prostaglandin synthesis by inhibiting the cyclo-oxygenase (COX) enzyme. KTP exhibits analgesic, antipyretic, and anti-inflammatory properties through non-specific COX-1 and COX-2 inhibition, thought to occur mainly in peripheral sites, although recent studies indicate that KTP also appears to have central effects [1]. KTP is a chiral molecule and only the S-enantiomer has beneficial biological activity [2]. Conditions causing elevated body temperature and acute pain (e.g. injury, illness, or medical procedures) are common in children, with NSAIDs frequently being used in children for the symptomatic treatment of fever and pain management. Pain in infants, children, and adolescents is often poorly assessed and managed [3]. Currently approved indications for KTP in adults include pain, fever, and certain inflammatory and musculoskeletal conditions. KTP is available in intravenous, intramuscular, oral (tablet and syrup), rectal, and topical formulations. In children, KTP has been investigated in postsurgical pain, predominantly in an intravenous formulation, although oral, intramuscular, and rectal formulations have also been investigated[4]. The oral tablet and syrup formulations have been assessed for use in fever and/or pain, and in inflammatory conditions. In pediatric patients, KTP is used for symptomatic relief of fever and management of pain in infants and children aged 6 months to 11 years (up to 35 kg). KTP is not approved for use in infants aged <6 months [5].

Therefore there is necessary to develop novel dosage forms such as nanosuspension. The nanosuspension can pass easily the first-pass metabolism. To enhance the therapeutic activity, the drug KTP was modified with novel technology and delivered through nanosuspension.

Thus, the nanosuspension formulation is one of the crucial formulations to enhance the therapeutic range of the drug and improve its bioavailability of the drug by reducing the dose [6]. A drug nanosuspension is characterized as finely colloid, biphasic, scattered, and strong medication particles [7]. A nanosuspension is prepared and balanced by stabilizers such as surfactants and cosurfactants [8]. The suspension has various applications by which the drug can deliver orally transdermal, ocularly, and parenterally [9]. For the nanosuspension drug delivery system the ideal nanoparticle size is 200-600 nm. The nanosuspension improves the solubility and bioavailability of the drug as well as improves the safety and efficacy of the drug molecules[7]. The nanosuspension can be produced with the help of micro fluidization and piston-gap homogenizers [9]

This process permits the micronization of drug particles to the submicron level [10]. To prepare nanosuspension, a very simple process is performed and more suitable for laboratory investigation[11].

Thus, in the present paper, we developed nanosuspension using the precipitation-ultrasonication method. In this work, we have applied CCD in which the experimental variables such as probe sonication time and total surfactant concentration influence the responses such as particle size, PDI, and EE (%). Optimization of the formulation was obtained using graphical and numerical methods to obtain the best formulation. There is no report has been published before this to improve the solubility and bioavailability using nanosuspension. The prepared KTP-loaded nanosuspension was lyophilized to obtain the dry nanosuspension. The dry nanosuspension was used for further characterization and evaluation.

## 2. MATERIALS AND METHODS

### 2.1. Materials

Ketoprofen (KTP) was kindly provided as a gift sample by Anant Pharmaceuticals Pvt. Ltd. (India). The surfactant, polysorbate 80 (Tween 80), and polyvinyl pyrrolidone K-30 (PVP K-30) were provided by (Loba Chemie Pvt Ltd, Mumbai) India. KCl was purchased from Qualigens fine chemicals, Navi Mumbai, India. NaOH was procured from S. D. Fine Chemicals, Mumbai, India. Methanol, acetonitrile, ethanol, and HCL were purchased from Rankem Ltd. India. Dimethyl Sulfoxide (DMSO) was purchased from S. D. Fine Chemical, Mumbai. Pure and Double distilled and filtered water (DDW) was prepared in the laboratory. All the other chemicals were off (AR grade) and required reagents procured and used in our experiment without re-purification.

### 2.2. Screening and selection of stabilizer

#### a) Based on solubility

The solubility of KTP in surfactant was determined using a flask-shake method previously reported [12]. The stabilizers from different categories such as non-ionic stabilizers (Poloxamer-188, tween 80), polymeric stabilizers (PVP-K30, HPMC), and anionic stabilizers (SLS) were evaluated. Briefly, the excess amount of KTP was added to the surfactant solution (4 mL) and shaken on the orbital shaker solution at the speed of 20 rpm for 48 h. Afterwards, the filter sample and separate the filtrate. Then undissolved KTP was separated from the filtrate. An aliquot sample of the filtrate was diluted with methanol and analyzed by a UV spectrophotometer.

#### b) Based on the particle size

The stabilizer was screened by the particle size measuring after the experiment run [12]. In brief, 0.5 % w/v of KTM in methanol was prepared. The stabilizer combination of 0.4 % Tween 80 and 0.2 % PVP K-30 was dissolved in the water and sonicated subsequently. The KTP-loaded nanosuspension was prepared as per the procedure and consequently characterized for particle size and PDI by zeta sizer. Each reading was taken in triplicate.

### 2.3. Preparation of KTP-loaded nanosuspension

Nanosuspension was prepared by the precipitation–ultrasonication method [12]. The drug (KTP) was dissolved in methanol by sonication for 5 min at room temperature. Different combinations of stabilizers were dissolved in water to obtain a series of antisolvent. Both solutions were passed through a 0.45 $\mu$ m filter. The antisolvent was cooled to 3°C in an ice-water bath. Then, the drug solution was quickly introduced utilizing a syringe positioned with the needle directly into the stabilizer solution into 40 mL of the pre-cooled antisolvent at different stirring speeds under the overhead stirrer to allow the volatile solvent to evaporate at room temperature for 4-5 hours. After the precipitation of antisolvent, the sample was immediately transferred to a test tube and was treated with an ultrasonic probe at different time lengths (in min). The probe with a tip diameter of 6 mm was immersed in the liquid, resulting in the wave travelling downwards and reflecting upwards. The period of ultrasound burst was set at 30:05 on:

off cycles and irradiated with the various amplitude of ultrasonic intensity. Further, nanosuspension was centrifuged at 10,000 RPM for 20 min (AllegraTM, 64R Centrifuge, Beckman, Coulter, USA) to concentrate the formulation [12]. The batch size for the preparation of nanosuspension was taken 40 mL. The physical mixture was prepared as an optimized formulation by the same method.

### 2.4. Design of experiment (DoE) for preparation of nanosuspension

The experimental trial was performed and after a successful trial we used a central composite design for the preparation of nanosuspension and to see the effect of experimental variables on the responses. Here CCD was applied by using the Design Expert software (version 11). The Alpha value was set and a total of 13 experimental runs were conducted with three variables which were coded at three levels, high (+1), medium (0), and low (-1).

Independent variables including the concentration of surfactant % (X1) and time of probe sonication % (X2) were studied at five different concentrations coded as  $-\alpha$ , -1, 0, 1, and  $+\alpha$ . The value for alpha is calculated to fulfil both rotatability and orthogonality in the design. All independent variables, their levels along with actual and coded values of these variables are shown in (Table 1). Whereas mean particle size (Y1), PDI (Y2), and EE% (Y3) were selected as response parameters as the dependent variables.

**Table 1. The coded and actual values of the variables used in CCD-RSM of KTP-nanosuspension**

Independent variables	Levels		
	Low (-1)	Middle (0)	High (+1)
X1: Conc. Of Surfactant	1.5	2	2.5
X2: Time of probe sonication	10	15	20
Dependent variables	Constraints		
Y1: Particle size (nm)	Minimum		
Y2: PDI (mV)	Minimum		
Y3: Entrapment efficiency (%)	Maximum		

All experimental runs were performed to find out the effect of experimental factors on their response. Here each response was expected to predict the model.

### 2.5. Statistical data analysis

Here, formulation variables are total surfactant concentration (X1) and probe sonication time (X2) respectively. The responses are the particle size (Y1), PDI (Y2) and entrapment efficiency (Y3). The CCD has five different levels ( $-\alpha$ , -1, 0, +1,  $+\alpha$ ) to study the effect of the variables. The various formulation run was displayed in Table 2

**Table 2: Formulation variables and their responses using CCD**

Run	Formulation variables		Response		
	Concentration of surfactant (%) (X <sub>1</sub> )	Time of probe sonication (min) (X <sub>2</sub> )	Particle size (nm) (Y <sub>1</sub> )	PDI (Y <sub>2</sub> )	EE (%) (Y <sub>3</sub> )
1	2	15	170.2	0.231	94.4

2	1.5	10		241.2	0.312	87
3	2.5	20		162.2	0.232	94
4	2	7.928932		189.2	0.326	89.23
5	2.5	10		165.3	0.437	97
6	2.707107	15		193.2	0.203	97.22
7	2	15		198.2	0.271	95.31
8	2	15		198.2	0.251	89.25
9	2	15		239.6	0.227	92
10	1.5	20		239.3	0.212	81.2
11	1.292893	15		413.2	0.221	63
12	2	22.07107		198.2	0.211	83
13	2	15		201.2	0.232	82.9

Mean  $\pm$  SD, (n=3); Coded high values=(-1), Coded middle/mean values=(0), Coded low values=(+1).

## 2.6. Response surface model and ANOVA

Using design expert software (version 7.0.0; Stat-Ease, Inc., Minneapolis, Minnesota, USA), the best model was predicted for all the responses. The effect of independent variables on the responses was calculated by ANOVA through Fisher's test. The P value less than 0.05 were considered to be statistically significant. Further, statistical analysis and graph plotting such as contour plots and 3D response surface plots were obtained.

## 2.7. Characterization of KTP-Nanosuspension

### 2.7.1. Determination of particle size and polydispersibility index (PDI)

The particle size analysis of KTP-nanosuspension was performed by photon correlation spectroscopy (PCS) using Zetasizer (Nano ZS 90, Malvern Instruments, UK) at a fixed angle of 90° at temperature of 25 °C. The Nanosuspension was diluted with distilled water before analysis. The PCS yielded the mean diameter (size) of the main population and PDI is a measure of the width of the particle size distribution[13]. This experiment was run in triplicate (n=3)

### 2.7.2. Zeta potential of the KTP-Nanosuspension

Zeta potential measurements were run at 25°C with an electric field strength of 23 V/m, using Zetasizer (Nano ZS 90, Malvern Instruments, UK). To determine the zeta potential, samples of KTP-nanosuspension were diluted and placed in electrophoresis cells. The zeta potential was calculated as described by Helmholtz–Smoluchowski equation[14]. The experimental was run in triplicate (n=3).

### 2.7.3. Determination of entrapment efficiency (EE %)

The % EE of KTP-nanosuspension was calculated by measuring the concentration of the untrapped or free drug in suspension [13]. About 2 mL of the suspension was placed in the Eppendorf tubes and

centrifuged at 15,000 rpm for 45 min at 4 °C (Remi Instruments Ltd., Mumbai, India). The amount of KTP in the aqueous phase was estimated spectrophotometrically at  $\lambda_{max}$  of 260 nm. The EE % of all formulated batches was calculated using the following Equations.

$$EE (\%) = [(W_{Total} - W_{Free})/W_{Total}] \times 100 \dots \dots \dots \text{Eq. (1)}$$

Where,  $W_{Total}$ ,  $W_{Free}$ , and  $W_{Lipid}$  are the weight of the total drug in suspension, the weight of the free drug in the aqueous phase, and the weight of the lipid used in the system, respectively.

## 2.8. Optimization of formulation

For optimization data analysis, the Design-Expert (version 7.0.0; Stat-Ease, Inc., Minneapolis, Minnesota, USA) was used in which graphical and numerical methods were used in which contour and 3D response surface plots were generated and used to optimize the formulation [15].

## 2.9. Lyophilization of KTP-Nanosuspension

The KTP-nanosuspension with added 2.5 % cryoprotectant (Mannitol) was frozen in a refrigerator at -75 °C for 24 hours [16]. Then the samples were lyophilized using a lab freeze-dryer (VirTis Benchtop K, SP scientific, Warminster USA). The freeze-drying was conducted for 68 to 72 h. After this, the vials were sealed with rubber caps.

## 2.10. Redispersibility of the nanosuspension

The freeze-dried nanosuspension of 100 mg was redispersed in 10 mL of double distilled water in a bottle with a cap. It was then shaken to disperse the particles in the water. It was then used for particle size, PDI, and surface charge as described in sections 2.7.1, and 2.7.2.

## 2.11. Solid state characterization of KTP-Nanosuspension

### 2.11.1. Differential scanning calorimetry (DSC) studies



DSC analysis was carried out using a differential scanning calorimeter (DSC 1 STAR the system, Mettler-Toledo, Switzerland). For DSC measurement; a scan rate of 10°C/min was employed over the heating rate range of 30–300 °C under a nitrogen purge. DSC studies were conducted for KTP, a physical mixture of KTP and surfactant, and dry nanosuspension of the optimized batch[17].

### 2.22.2. X-ray diffraction (XRD)

Crystalline structures of the suspension were investigated using XRD (Bruker AXS D8 Advance, Germany). The samples were mounted on a sample holder and XRD patterns were scanned in the range of 3–80° at a chart speed of 5 °C per min. Samples used for measurement were pure KTP, a physical mixture of KTP and surfactant, and dry nanosuspension of the optimized batch [15].

### 2.22.3. Scanning electron microscopy (SEM)

The surface morphology of the suspension was studied by SEM [17]. The optimized formulation was kept on the metal plate and dried under vacuum to form a dry film which was then observed under the SEM (LEO 440i; Leo Electron Microscopy Ltd., Cambridge, UK).

## 2.12. *In vitro* release study of an optimized batch of KTP-nanosuspension

It is usually known that the release of the drug from nanocarriers is influenced by various factors such as the structure and composition of the nanosuspension. The *in vitro* releases of KTP from developed nanosuspension was studied [18].

*In vitro* release of KTP was performed in pH 1.2 HCL and phosphate buffer saline solution (PBS) pH 6.8, using a dialysis bag technique. The dialysis bags were hydrated in phosphate-buffered saline, pH 6.8 overnight before the experiment. nanosuspension containing Ketoprofen was placed in dialysis bags. The dialysis bags were tied at both ends and were placed in the beaker containing 100 mL phosphate buffer saline pH 6.8 after pH 1.2 HCL. The beaker was maintained at 37±2°C and stirred at a constant speed of 100 rpm[19]. The sample was withdrawn at regular intervals of 0, 0.5, 1, 2, 3, 4, 5, 6, 7, 8, 9, 10, 11, 12, and 24 h. The study was conducted in pH 1.2 HCL for the first 2 h and then pH 6.8 for the next 24 h. The sample of 3mL of dissolution medium was removed and was replaced with the fresh buffer at the same temperature to maintain sink condition. The amount of KTP in the aliquots was analyzed by

UV-visible spectrophotometer (UV 1700, Shimadzu, Japan) at  $\lambda_{max}$  260 nm.

## 3. RESULTS AND DISCUSSION

For designing KTP-nanosuspension, total surfactant concentration was used in the range of 1.5 to 2.5 and the time of the probe sonication was kept at 10 to 20 min to get results of the desired response.

Here, the main factor that affected the PS, PDI and EE of the KTP-nanosuspension. Total surfactant concentration ( $X_1$ ), and time of the probe sonication ( $X_2$ ) as Independent variables and mean PS ( $Y_1$ ), PDI ( $Y_2$ ), and EE ( $Y_3$ ), are the dependent variables. The change in the concentration of independent variables changes the responses. As PS, PDI decreases when surfactant concentration and concentration of lipids increase and EE increases. Thus, depending upon the result obtained the optimal range of independent variables concentration of surfactant 1.5-2.5 (%) and the time of probe sonication 10 -20 min.

### 3.1. DoE approach for the formulation

The most important factors influencing nanosuspension are particle size, PDI and EE. The most popular Central Composite design was used to determine the optimum levels of these variables. The central composite design response surface methodology (CCD– RSM) constitutes an alternative approach because it offers the possibility of investigating a high number of variables at different levels with only a limited number of experiments [20]. **Table 2** shows the experimental results considering variables such as mean particle size of nanosuspension ( $Y_1$ ), PDI ( $Y_2$ ), and (EE %) of nanosuspension.

#### 3.1.1. Fitting of data to the model

The ranges of responses particle size,  $Y_1$ ; PDI,  $Y_2$  and EE%,  $Y_3$  were 162.2 to 413.2 nm, 0.203 to 0.437 and 63.0 to 97.22 % respectively. All the responses observed for 13 formulations prepared were fitted to various models using Design-Expert software. It was observed that the best-fitted models were Quadratic for the particle size and linear for PDI and EE%. The quadratic model was studied/selected because it shows the interactive effect of all the independent variables on responses that the linear/non-linear model does not show. Table 3 shows the summary of regression analysis for the responses such as particle size ( $Y_1$ ), PDI ( $Y_2$ ) and EE ( $Y_3$ ).

**Table 3 Summary of results of regression analysis for responses  $Y_1$ ,  $Y_2$  and  $Y_3$**

Models	R2 Value	Adjusted R2	Predicted R2	S. D	C.V. %

Particle size (Y1)	0.8037	0.6634	-0.1271	37.67	17.43
PDI (Y2)	0.5649	4779	0.0944	0.047	18.29
EE % (Y3)	0.6474	0.5769	0.3559	6.05	6.87

### 3.2. Effect of variables

#### 3.2.1. Particle size (PS):

The particle size is an important attribute of the nanosuspension formulation. This is the first response that we checked at the beginning. This was

found in the range of 162.2 to 413.2 (Table 2). Using ANOVA (Table 4) and statistical calculation it was found that the level of significance ( $p < 0.05$ ). the model was a quadratic model.

**Table 4: ANOVA for response measurement of Particle size (Y<sub>1</sub>), PDI (Y<sub>2</sub>), and EE (Y<sub>3</sub>)**

Source	Sum of squares	df	Mean square	F-value	p-value	
<b>Particle size (Y1)</b>						
Quadratic Model	40659.65	5	8131.93	5.73	0.0492	Significant
Residual	9933.18	7	1419.03			
Cor Total	50592.83	12				
<b>PDI (Y2)</b>						
Model	0.029	2	0.015	6.49	0.0156	Significant
Residual	0.022	10	2.243E-003			
Cor Total	0.052	12				
<b>EE (Y3)</b>						
Model	672.35	2	336.17	9.18	0.0055	significant
Residual	366.21	10	36.62			
Cor Total	1038.55	12				

df - Degree of freedom, F - Fisher's ratio, and  $p$ - probability ( $P < 0.05$ )

The particle size was shown in the following equation,

$$\text{Particle size} = 201.48 - 58.02 * X_1 + 0.97 * X_2 - 0.30 * X_1 * X_2 + 39.25 * X_1^2 - 15.50 * X_2^2 \dots\dots\dots(1)$$

The above equation provides an idea about the effect of the formulation variables on the response of particle size. Analysis of particle size denotes the negative relationship between particle size and total surfactant concentration. As the surfactant concentration increases the particle size decreases. The positive relationship between probe sonication time and particle size. so probe sonication time should be moderate. Thus increase in probe

sonication time increases the collision of the particles and increases the particle size.

#### 3.2.2. Polydispersity Index (PDI)

The PDI is an important attribute of nanosuspension. The uniformity of the particles of nanosuspension is identified by the polydispersity index. The 2 D and 3 D of the image was shown in Fig. 1. The range of the PDI was found to be 0.203 to 0.437 indicating uniformity and homogeneity of the particles. The model was found to be linear and level of significance ( $< 0.05$ ). The model equation is given below:

$$\text{PDI} = 0.26 + 0.015 * X_1 - 0.058 * X_2 \dots\dots\dots(2)$$

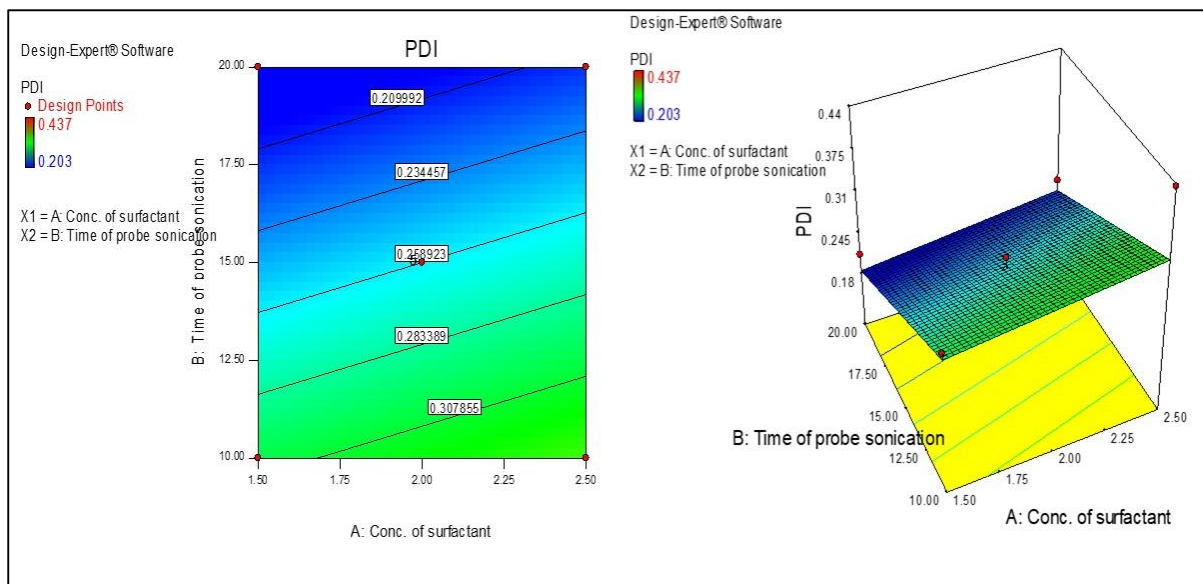


Fig. 1. Response surface plot showing the effect of total surfactant concentration (X<sub>1</sub>) and time of probe sonication (X<sub>2</sub>) on the PDI

A polynomial equation of the PDI described that the increase in surfactant concentration increases the PDI. On the other hand time of the probe, sonication has a negative relationship with PDI. That means decreases the time of probe sonication and increases the PDI. Hence it should be moderate.

[21]. The EE described the amount of the drug encapsulated in the particles. The 2 D and 3 D images of the response of the image was shown in Fig. 2. The range of the EE was found to be 63 – 97.22 %. The following equation shows the linear model with a level of significance < 0.05.

### 3.2.3. Entrapment efficacy (EE)

The EE denotes the entrapment of the drug particles in the lattice arrangement of the nanosuspension

$$\% \text{ EE} = 88.12 + 8.90 * X_1 - 2.20 * X_2 \dots\dots\dots(3)$$

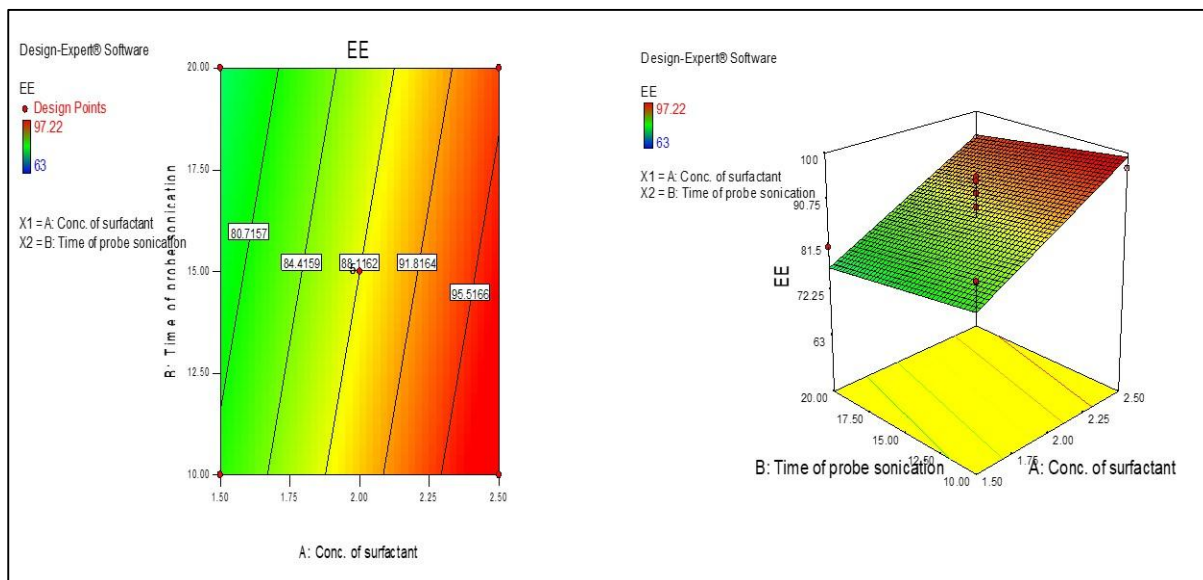


Fig. 2. Response surface plot showing the effect of total surfactant concentration (X<sub>1</sub>) and time of probe sonication (X<sub>2</sub>) on the EE (%)

The above equation indicates that the increase in surfactant concentration increases the % entrapment. At the same time, if a decrease in probe sonication time gradually increases the % EE. This is because the particles could not burst in low location time.

The entrapment can be affected with the help of the surfactant concentration and its combination.

### 3.2.4. Optimization of the formulation of KTP–nanosuspension

The optimized formulation of KTP-Nanosuspension was selected by using Design-Expert (version 7.0.1, Stat-Ease, Inc., Minneapolis, MN, USA) software. Criteria of variables were selected as maximum % EE, minimum mean particle size, and PDI within the specified range for optimization. Depending upon the criteria selection software provides solutions for the selection of optimized formulations. Most probable

optimal formulation KTP-Nanosuspension was selected with a total surfactant Concentration of 2.50% and a Probe sonication time of 20 min. The optimized formulation of KTP-Nanosuspension was prepared and characterized. The experimental and predicted values for the most probable optimal formulation of KTP-nanosuspension was shown in Table 5.

**Table 5: Comparison between the experimental and predicted values for the most probable optimal formulation of KTP-nanosuspension**

Dependent variable	Optimized nanosuspension formulation	
	Experimental	Predicted
Particle size(nm) Y1	169.2	176.402
PDI Y2	0.303	0.284
EE (%) Y3	97.22	95.64

### 3.3 Physicochemical characterization

#### 3.3.1 Particle Size and Polydispersity Index of KTP-nanosuspension

The major objective of using general optimal design was to determine the levels of the two factors i.e. Surfactant Concentration (%) (X1) and time of probe sonication (X2) which produces the nanosuspension with minimum particle size and maximum entrapment efficiency. The particle size of the nanosuspension is a crucial factor because it determines the rate and extent of drug release as well as drug absorption. The smaller droplet size provides a larger interfacial surface area for drug absorption. In addition, it was suggested that the smaller droplet size permits a faster release rate. Also, it has been reported that the smaller particle size of the emulsion

droplets may lead to more rapid absorption and improve bioavailability. Also, PDI measures the width of particle size distribution. If PDI is lower than 0.1, it might be associated with high homogeneity in the particle population, whereas high PDI values suggest a broad size distribution. The particle size and polydispersity index (PDI) of the fabricated batches were in the range of 162.2 to 413.2 nm, and 0.203 to 0.437 respectively (Figure 3). The particle size obtained in the present study is within the size range (162.2 to 413.2 nm) required for efficient lymphatic uptake, therefore, it may be expected that the size is acceptable and would not be a limiting factor in the lymphatic uptake of the prepared nanosuspension.

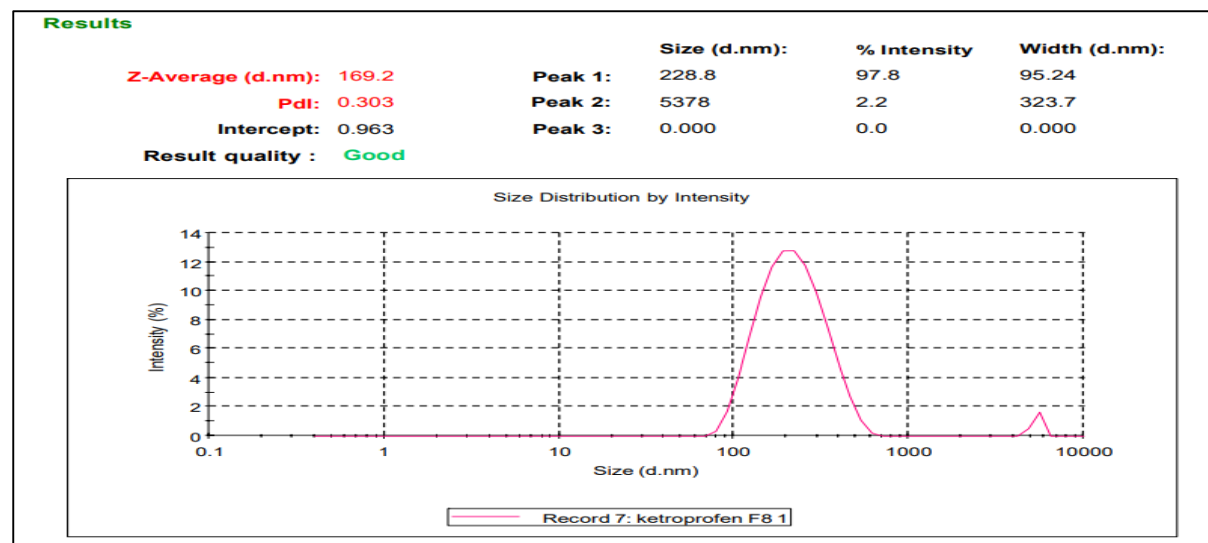


**Fig 3: Particle size and Polydispersity index of KTP-nanosuspension**

#### 3.3.2. Entrapment efficiency (EE %) of the KTP-nanosuspension.

10 different batches of nanosuspension were prepared by varying the lipid concentrations. The amount of drug was kept constant for all the batches.



The entrapment efficiency of all the batches ranges from 87 % to 97.22 % respectively. Such a high value of entrapment efficiency may be due to the highly lipophilic nature of the drug KTP and its high solubility in GMS.

### 3.5 Lyophilization of KTP –nanosuspension

The nanosuspension was successfully freeze-dried using the bench-top freeze dryer. Lyophilization was carried out for the optimized batch at  $-75^{\circ}\text{C}$  with 2.5 % mannitol as a cryoprotectant. The role of cryoprotectant is to decrease Nanoparticle aggregation during the process of freeze-drying. The obtained lyophilized powder was found to be dry, porous and friable after 72 h. The vacuum was maintained at 76 mTorr.

### 3.5 Solid state characterization of optimized nanosuspension

#### 3.5.1 Differential Scanning Calorimetry

The DSC thermograms of bulk KTP, lyophilized nanosuspension are shown in Fig. 4. KTP showed a characteristic sharp endothermic peak at  $94^{\circ}\text{C}$  and the lyophilized KTP-nanosuspension showed a very small and not sharp endothermic peak around  $97.49^{\circ}\text{C}$  (C). This small and not sharp endothermic peak indicates that few traces of KTP may present in KTP-nanosuspension and most KTP molecules converted from the crystalline form of the drug to the amorphous form i.e.maximum entrapment of KTP in the lipid matrix. It was also concluded that KTP is molecularly dispersed in the lipid matrix, indicating its reduction in crystallinity as the peak intensity of the drug was found to be reduced [22].

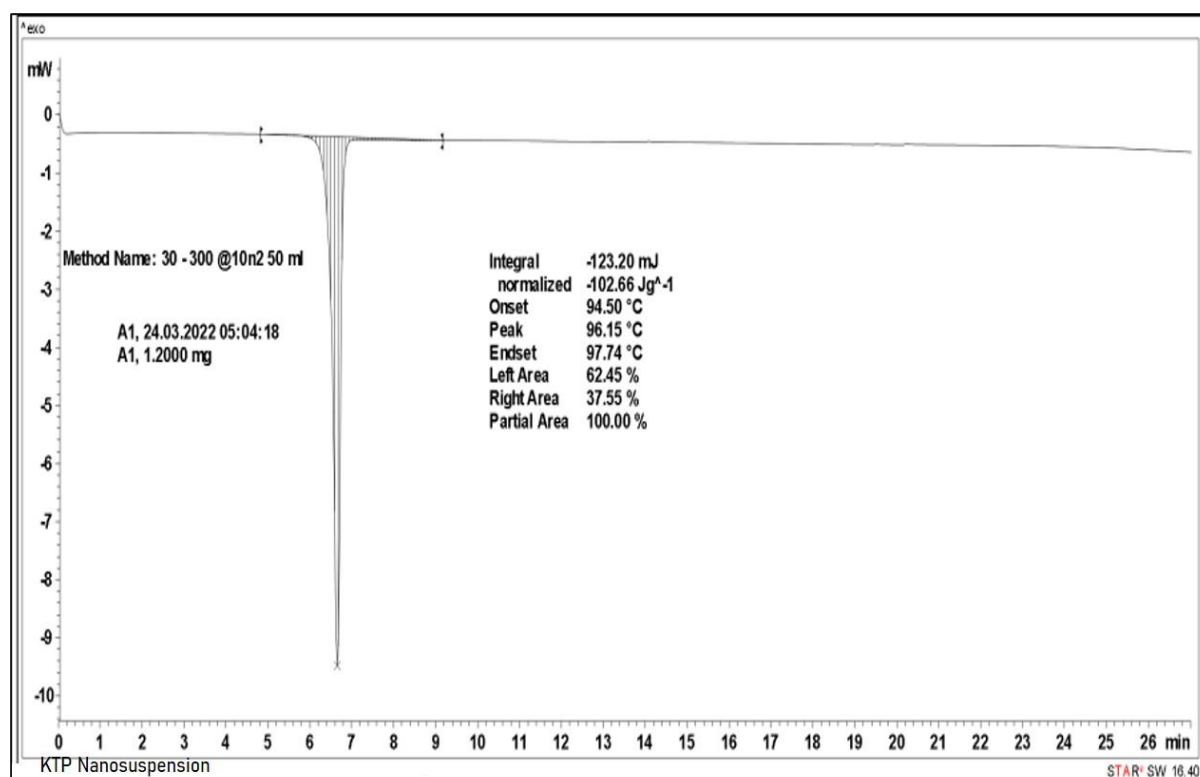


Fig. 4. DSC pattern of the drug-loaded lyophilized nanosuspension formulation.

#### 3.5.2. X-ray diffraction studies

X-ray diffraction patterns of the pure crystalline drug, physical mixture of drug and lyophilized nanosuspension formulation are shown in Fig. 5. The typical crystalline nature of the drug was defined by observing sharp principal peaks of KTP between 5 to 50 on  $2\theta$  scales. The  $2\theta$  scattered angle of the drug was found to be  $6.384^{\circ}$ ,  $11^{\circ}$ ,  $14.401^{\circ}$ ,  $18.353^{\circ}$ , and  $22.807^{\circ}$ . Distinctive sharp peaks of

drug disappeared in drug-loaded freeze-dried nanosuspension formulation[23]. The scale of the formulation was found to be  $13.171^{\circ}$ ,  $14.397^{\circ}$ ,  $18.378^{\circ}$ , and  $22.811^{\circ}$  although both broad peak and sharp peak were obtained in the physical mixture of drug. These results were in good support with DSC results, indicating the KTP conversion of crystalline to amorphous state[24].

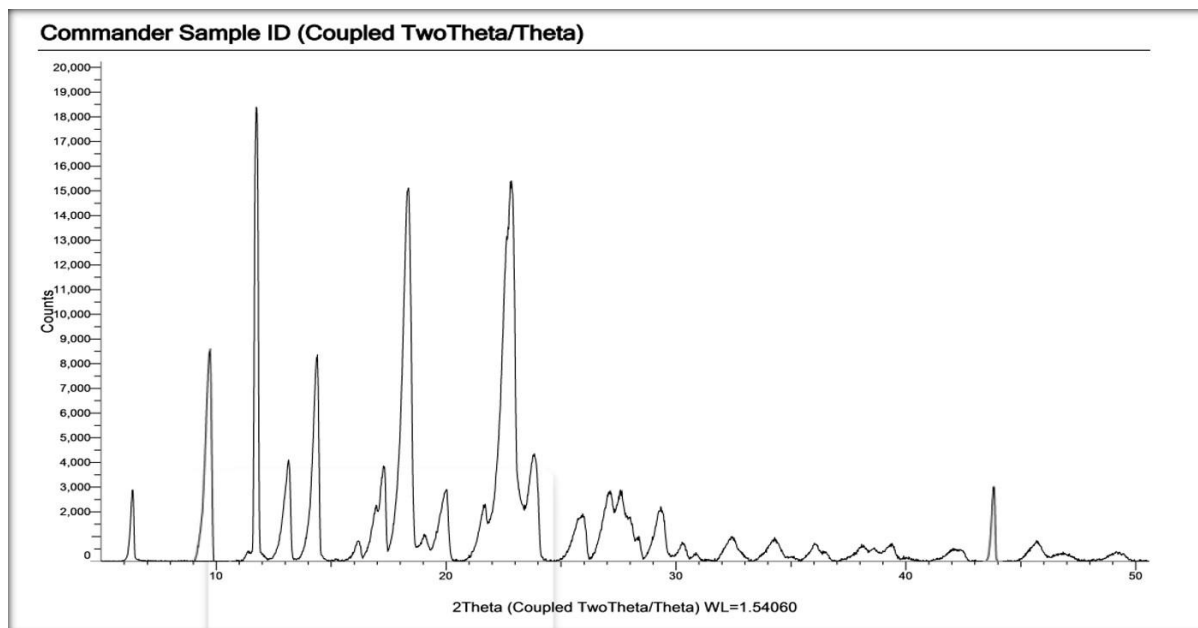


Fig. 5. XRD pattern of the drug-loaded lyophilized nanosuspension formulation.

### 3.5.3 Fourier transform infrared spectroscopy (FTIR)

FTIR spectra for KTP, optimized KTP-Nanosuspension batch were depicted in Fig. 6. IR spectra displayed the peak range at  $1697.41\text{ cm}^{-1}$ ,  $717.54\text{ cm}^{-1}$ ,  $1458.23\text{ cm}^{-1}$ ,  $2644.49\text{ cm}^{-1}$ , is attributed to C=O stretching; C-H bending; C=C stretching; COOH stretching. Thus, the assigned peak confirmed the structure of KTP. The IR spectrum of a physical mixture at  $2922.25\text{--}2850.88\text{ cm}^{-1}$ ,  $1745.64\text{ cm}^{-1}$ , and  $1467.88\text{ cm}^{-1}$  could be designated to  $\text{SP}^3$  C-H stretching, CO, stretching, and methyl -CH, deformation vibration. In this

study, the drug does not show an absorption band in the fingerprint scan of the IR spectrum of the Physical mixture due to the complete conversion of drug molecules into the amorphous form of KTP in the melted sample. This is further confirmed through the results of DSC and PXRD. An optimized KTP-nanosuspension shows the absorption band in the IR spectrum at  $2922.25\text{--}2850.88\text{ cm}^{-1}$ ,  $1745.64\text{ cm}^{-1}$ ,  $1467.88\text{ cm}^{-1}$  recognized to  $\text{SP}^3$  C-H stretching, CO, stretching, methyl CH, deformation vibration respectively. The intensity of the absorption peak was reduced and shortened due to complete conversion into an amorphous form.

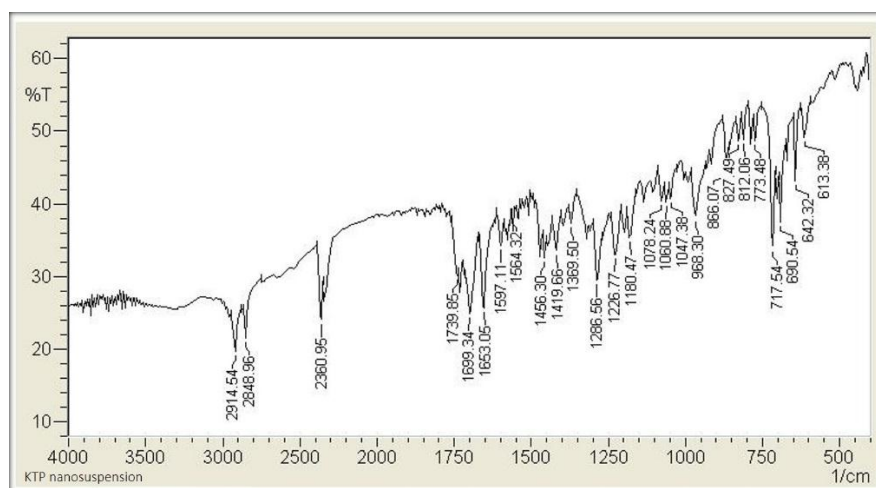


Fig. 6. FTIR spectra of the drug-loaded lyophilized nanosuspension formulation.

### 3.5.4 Scanning Electron Microscopy

A morphological study of optimum formulation was done by taking SEM pictures of prepared nanosuspension. It was revealed that they were uniformly distributed (Fig. 7). Studies also verified that the crystalline KTP is converted to its

amorphous form as it was encapsulated by lipids. Studies showed that the predicted particle size and measured size with a zeta sizer were comparable with the size of particles that were observed by SEM.

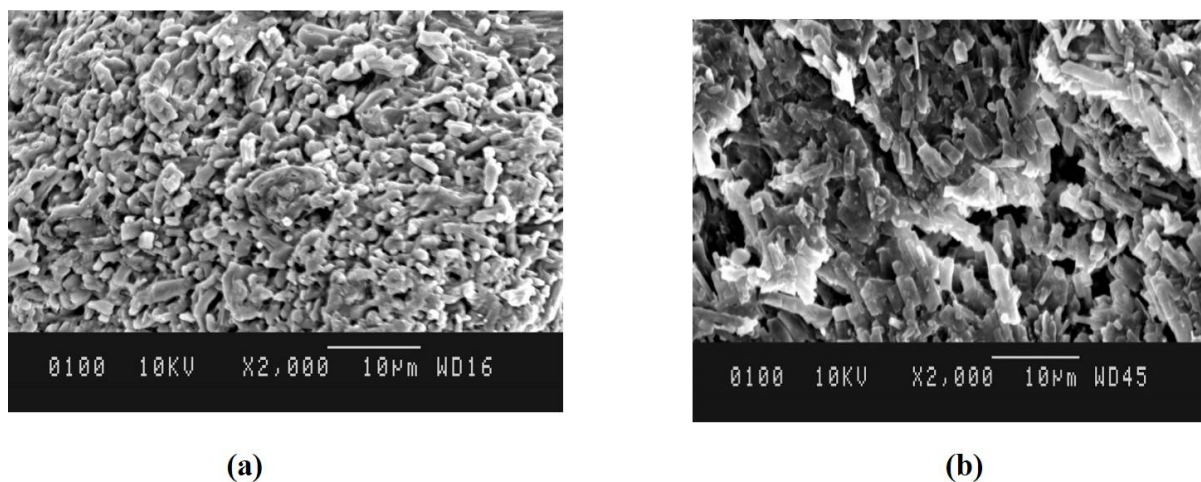


Fig. 7. SEM of the pure drug (a) & Ketoprofen- nanosuspension (b)

### 3.6 *In vitro* release study of an optimized batch of KTP-nanosuspension

The *in vitro* dissolution profile was described in Fig. 8. In comparison, 30 % drug was released in less than 1 hr for lyophilized KTP-nanosuspension while API-suspension takes released only 10 % drug in 1 h. the release of the drug from the nanosuspension is due to the surfactant Tween 80 present in the suspension. The poor drug release from the API suspension was attributed to the poorly aqueous soluble drug, poor wettability, and maybe aggregation of the particles. The increase in the drug release was due to the combination of the surfactant

present in the nanosuspension [25]. In addition, the increase in drug dissolution rate was due to the size reduction of the nanosuspension. The reduction in size of the particle increases the surface area and thus, enhancement of the bioavailability of the KTP. Moreover, drug particles were converted into amorphous during the process. And this is the reason for the improvement of the dissolution behavior of the nanosuspension. For the comparison of the mechanism of release kinetics, the Korsmeyer-Peppas release kinetics was found to be the best-fit model correlation coefficient ( $r^2= 0.8956$ ).

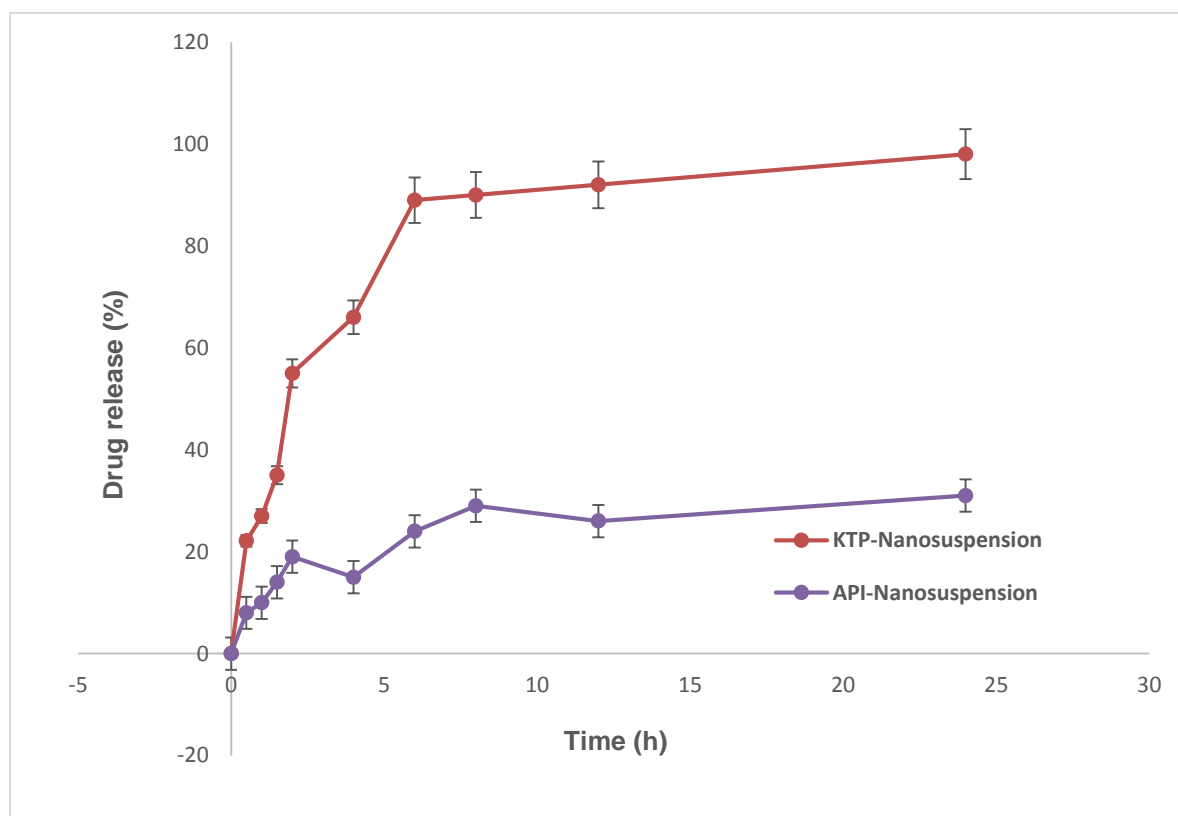


Fig. 8. *In vitro* release study of lyophilized KTP nanosuspension and the API suspension

#### 4. CONCLUSION

The present work deals with KTP loaded with nanosuspension to improve solubility and bioavailability. The design of the experiment i.e. CCD was helpful to find out the effect of variables on the responses. The physicochemical characterization was performed on the optimized nanosuspension for the observation of the performance of the formulation. The DSC and PXRD studies showed that the drug was crystalline before the processing and transform into an amorphous nature after the processing. The compatibility study was performed using the FTIR study. An improved solubility was obtained using present nanosuspension. The outcome of this nanosuspension formulation is to produce cost-effective and potential nanoformulations to reduce pain. Thus, using nanoformulations, we can improve the solubility and bioavailability of the lipophilic drug. The nanosuspension formulation can be taken on a large scale in the future.

#### Acknowledgement

We would like to express our sincere gratitude to Sunrise University, Alwar Pharmacy College, Alwar, Rajasthan, India for providing us with the research facility required to conduct our study. The support extended by the institution was instrumental in completing the research project. We also thank the faculty members and staff for their cooperation and assistance throughout the project. Their guidance and expertise were invaluable in shaping the research direction and methodology. We are grateful for the opportunity to have access to the facilities and resources provided by Sunrise University, Alwar Pharmacy College.

#### Conflict of Interest:

No Conflict of interest

#### 5. REFERENCES

1. N.K. Yadav, S. Nanda, G. Sharma, O.P. Katare, Systematically Optimized Ketoprofen-Loaded Novel Proniosomal Formulation for Periodontitis: In Vitro Characterization and In Vivo Pharmacodynamic Evaluation, *AAPS PharmSciTech.* 18 (2017) 1863–1880. <https://doi.org/10.1208/s12249-016-0665-1>.
2. D. Mou, H. Chen, J. Wan, H. Xu, X. Yang, Potent dried drug nanosuspensions for oral bioavailability enhancement of poorly soluble drugs with pH-dependent solubility, *Int. J. Pharm.* 413 (2011) 237–244. <https://doi.org/10.1016/j.ijpharm.2011.04.034>.
3. M. Cirri, M. Bragagni, N. Mennini, P. Mura, Development of a new delivery system consisting in “drug – in cyclodextrin – in nanostructured lipid carriers” for ketoprofen topical delivery, *Eur. J. Pharm. Biopharm.* 80 (2012) 46–53. <https://doi.org/10.1016/j.ejpb.2011.07.015>.
4. P. Chattopadhyay, B.Y. Shekunov, D. Yim, D. Cipolla, B. Boyd, S. Farr, Production of solid lipid nanoparticle suspensions using supercritical fluid extraction of emulsions (SFEE) for pulmonary delivery using the AERx system, *Adv. Drug Deliv. Rev.* 59 (2007) 444–453. <https://doi.org/10.1016/j.addr.2007.04.010>.
5. H. Kokki, Ketoprofen pharmacokinetics, efficacy, and tolerability in pediatric patients, *Pediatr. Drugs.* 12 (2010) 313–329. <https://doi.org/10.2165/11534910-000000000-00000>.
6. R. Jayaprakash, K. Krishnakumar, B. Dineshkumar, R. Jose, S.K. Nair, Nanosuspension in Drug Delivery-A Review, *Sch. Acad. J. PharmacyOnline) Sch. Acad. J. Pharm.* 5 (2016) 2320–4206. [www.saspublisher.com](http://www.saspublisher.com).
7. K.B. Sutradhar, S. Khatun, I.P. Luna, Increasing possibilities of nanosuspension, *J. Nanotechnol.* 2013 (2013). <https://doi.org/10.1155/2013/346581>.
8. S. Jacob, A.B. Nair, J. Shah, Emerging role of nanosuspensions in drug delivery systems, *Biomater. Res.* 24 (2020). <https://doi.org/10.1186/S40824-020-0184-8>.
9. Y. Wang, Y. Zheng, L. Zhang, Q. Wang, D. Zhang, Stability of nanosuspensions in drug delivery, *J. Control. Release.* 172 (2013) 1126–1141. <https://doi.org/10.1016/j.jconrel.2013.08.006>.
10. T. Venkatesh, A.K. Reddy, J. Uma Maheswari, M. Deena Dalith, C.K. Ashok Kumar, Nanosuspensions: Ideal approach for the drug delivery of poorly water soluble drugs, *Der Pharm. Lett.* 3 (2011) 203–213.
11. Y. Ma, Z. Cong, P. Gao, Y. Wang, Nanosuspensions technology as a master key for nature products drug delivery and In vivo fate, *Eur. J. Pharm. Sci.* 185 (2023) 106425. <https://doi.org/10.1016/j.ejps.2023.106425>.
12. P. Shekhawat, V. Pokharkar, Risk assessment and QbD based optimization of an Eprosartan mesylate nanosuspension: In-vitro characterization, PAMPA and in-vivo assessment, *Int. J. Pharm.* 567 (2019) 118415. <https://doi.org/10.1016/j.ijpharm.2019.06.006>.
13. V.C. Gurumukhi, S.B. Bari, Quality by design (QbD)-based fabrication of atazanavir-loaded nanostructured lipid carriers for lymph targeting: bioavailability enhancement using chylomicron flow block model and toxicity studies, *Drug Deliv. Transl. Res.* (2021). <https://doi.org/10.1007/s13346-021-01014-4>.
14. S. Das, W.K. Ng, R.B.H. Tan, Are nanostructured lipid carriers (NLCs) better than

- solid lipid nanoparticles (SLNs): Development, characterizations and comparative evaluations of clotrimazole-loaded SLNs and NLCs?, *Eur. J. Pharm. Sci.* 47 (2012) 139–151. <https://doi.org/10.1016/j.ejps.2012.05.010>.
15. V.C. Gurumukhi, S.B. Bari, Development of ritonavir-loaded nanostructured lipid carriers employing quality by design (QbD) as a tool: characterizations, permeability, and bioavailability studies, *Drug Deliv. Transl. Res.* (2021). <https://doi.org/10.1007/s13346-021-01083-5>.
  16. V.C. Gurumukhi, S.B. Bari, Fabrication of efavirenz loaded nano-formulation using quality by design (QbD) based approach: Exploring characterizations and in vivo safety, *J. Drug Deliv. Sci. Technol.* 56 (2020) 101545. <https://doi.org/10.1016/j.jddst.2020.101545>.
  17. D.N. Tapre, S.P. Borikar, S.P. Jain, S.R. Walde, G.G. Tapadiya, V.C. Gurumukhi, Development and evaluation of novel famotidine-loaded fast dissolving sublingual film using the quality-by-design approach, *J. Drug Deliv. Sci. Technol.* 85 (2023) 104581. <https://doi.org/10.1016/j.jddst.2023.104581>.
  18. S.S. Chalikwar, V.S. Belgamwar, V.R. Talele, S.J. Surana, M.U. Patil, Formulation and evaluation of Nimodipine-loaded solid lipid nanoparticles delivered via lymphatic transport system, *Colloids Surfaces B Biointerfaces.* 97 (2012) 109–116. <https://doi.org/10.1016/j.colsurfb.2012.04.027>.
  19. J. Hao, F. Wang, X. Wang, D. Zhang, Y. Bi, Y. Gao, X. Zhao, Q. Zhang, Development and optimization of baicalin-loaded solid lipid nanoparticles prepared by coacervation method using central composite design, *Eur. J. Pharm. Sci.* 47 (2012) 497–505. <https://doi.org/10.1016/j.ejps.2012.07.006>.
  20. V.C. Gurumukhi, S.B. Bari, Quantification and Validation of Stability-Indicating RP-HPLC Method for Efavirenz in Bulk and Tablet Dosage Form using Quality by Design (QbD): A Shifting Paradigm, *J. Chromatogr. Sci.* (2021) 1–14. <https://doi.org/10.1093/chromsci/bmab061>.
  21. V.C. Gurumukhi, V.P. Sonawane, G.G. Tapadiya, S.B. Bari, S.J. Surana, S.S. Chalikwar, Quality-by-design based fabrication of febuxostat-loaded nanoemulsion: Statistical optimization, characterizations, permeability, and bioavailability studies, *Heliyon.* 9 (2023) e15404. <https://doi.org/10.1016/j.heliyon.2023.e15404>.
  22. B. Shah, D. Khunt, H. Bhatt, M. Misra, H. Padh, Application of quality by design approach for intranasal delivery of rivastigmine loaded solid lipid nanoparticles : Effect on formulation and characterization parameters, *Eur. J. Pharm. Sci.* 78 (2015) 54–66. <https://doi.org/10.1016/j.ejps.2015.07.002>.
  23. J.K. Kim, J.S. Park, C.K. Kim, Development of a binary lipid nanoparticles formulation of itraconazole for parenteral administration and controlled release, *Int. J. Pharm.* 383 (2010) 209–215. <https://doi.org/10.1016/j.ijpharm.2009.09.008>.
  24. G. V. Patel, V.B. Patel, A. Pathak, S.J. Rajput, Nanosuspension of efavirenz for improved oral bioavailability: Formulation optimization, in vitro, in situ and in vivo evaluation, *Drug Dev. Ind. Pharm.* 40 (2014) 80–91. <https://doi.org/10.3109/03639045.2012.746362>.
  25. J. Luan, F. Zheng, X. Yang, A. Yu, G. Zhai, Nanostructured lipid carriers for oral delivery of baicalin : In vitro and in vivo evaluation, *Colloids Surfaces A Physicochem. Eng. Asp.* 466 (2015) 154–159. <https://doi.org/10.1016/j.colsurfa.2014.11.015>.